IEEE Access
Multidisciplinary ⋮ Rapid Review ⋮ Open Access Journal

Received 3 September 2024, accepted 8 October 2024, date of publication 11 October 2024, date of current version 25 October 2024.

Digital Object Identifier 10.1109/ACCESS.2024.3478812

RESEARCH ARTICLE

A 3 × 3 Antenna Beamforming Network Based on Waveguide Nolen Matrix for Ka-Bands

HATEM ODAY HANOOSH[1,2,3], MOHAMAD KAMAL A. RAHIM[1], (Senior Member, IEEE), NOOR ASNIZA MURAD[1], (Senior Member, IEEE), AND YAQDHAN MAHMOOD HUSSEIN[1,2,3]

[1]Advance RF and Microwave Research Group (ARFMRG), Faculty of Electrical Engineering, Universiti Teknologi Malaysia (UTM), Johor Bahru, Johor 81310, Malaysia
[2]Department of Electronics and Communication, College of Engineering, Al-Muthanna University, Samawah 66001, Iraq
[3]College of Engineering, Al Ayen University, Nasiriyah 64001, Iraq

Corresponding authors: Hatem Oday Hanoosh (hatem.altaee1990@gmail.com) and Mohamad Kamal A. Rahim (mkamal@fke.utm.my)

This work was supported in part by the Ministry of Higher Education (MOHE) under Fundamental Research under Grant FRGS/1/2021/STG04/UTM/01/1; and in part by the School of Postgraduate Studies (SPS), Research Management Centre, Advanced RF and Microwave Research Group, Faculty of Electrical Engineering, Universiti Teknologi Malaysia (UTM), Johor Bahru, under Grant 04M37.

ABSTRACT The Fifth generation (5G) wireless communication system aims to provide high bandwidth, high sensitivity, high gain and power capability. Millimeter wave technology then proposed for these demands with various range of features such as higher bandwidth, low interference, and frequency reuse. However, millimeter wave technology has a key disadvantage of high path loss due to small wavelength in the channel of high attenuation coming from the atmosphere, in addition to the very small wavelength that produces an unwanted crosstalk between the transmission lines. Thus, beamforming network and waveguide-based structures such as Nolen matrix was proposed to overcome these problems. The objective of this research is to design a low loss and high-performance Nolen beamforming network based on waveguide technology. Taking in consideration is the advantage of flexible number of beam ports in Nolen matrix using single layer technique. This work aims to design a 3 × 3 Nolen matrix with main beam directions of 0, 30° and −30° at 26 GHz. The 3 × 3 Nolen matrix is designed using low loss hollow waveguide single layer technique. Then, the proposed Nolen matrix is fed three-waveguide slotted antenna. The proposed 3 × 3 Nolen matrix has measured phase differences at port 1 (35.40°), port 2 (156.43°) and port 3 (−93.57°) in the x-y plane. Waveguide slotted antenna has designed at 26 GHz with tilted slots at broad wall of the waveguide structure. This tilted technique has the benefit of increasing the bandwidth up to 50% of FBW. A simulation and measurement using CST software is performed for the proposed antenna. A return loss of −15 dB with wideband of 2.08 GHz are obtained. A gain of 14 dB is observed at broad wall respectively. Waveguide antenna has been integrated with Nolen matrix to build Nolen beamforming; the measured beamforming network has a good return loss of less than - 10 dB with phase error of −8 degree at outputs. Three beams are achieved with beam scanning of ± 30 degree. The beam from port 1 is radiated in the direction of −26°. The beams from port 2 and port 3 are radiated in the directions of +27° and +6° respectively. Therefore, this beamforming has a greater impact on the mm wave beamforming networks and applications.

INDEX TERMS Nolen matrix, direct coupling, beamforming network, millimeter wave.

I. INTRODUCTION

Fifth generation (5G) technology aims to provide huge bandwidths and high data rates systems for current wireless applications. That is the major factor for shifting to higher frequency to provide that trend. Millimeter wave's (Mm-wave) bands then proposed as a powerful candidate for 5G wireless standards [1], [2], [3], [4]. Mm-wave technology was established few decades ago in purpose of military use and point to point communication applications [3]. Mm-wave

The associate editor coordinating the review of this manuscript and approving it for publication was Santi C. Pavone.

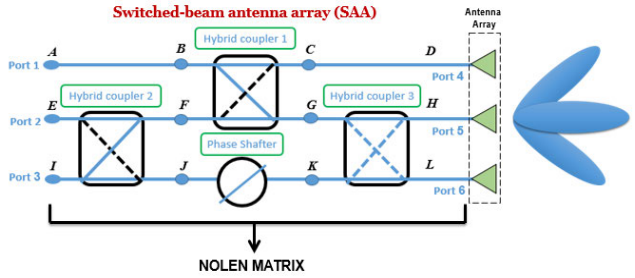

FIGURE 1. The proposed beamforming network with 3 × 3 Nolen Matrix.

TABLE 1. Path of input ports into output ports with phase difference.

Excited Port	Path	Output Ports	Phase Difference
Port 1	A, B, C, D	4	−90°
	A, B, G, H	5	
	A, B, G, L	6	
Port 2	E, F, G, H	4	+150°
	E, F, C, D	5	
	E, F, G, L	6	
Port 3	I, J, K, L	4	+30°
	I, F, G, H	5	
	I, J, K, L	6	

technology has the potential of providing high bandwidth up to 5 GHz beside the trending technologies of low-cost fabrication and low-loss materials [5], [6]. These trends shift the current researches forward to standardizing and licensing Mm-wave bands for 5G cellular networks in both commercial and industrial fields.

Mm-wave band starts generally from frequency spectrum of 30 GHz to 300 GHz, with a small operating wavelength ranging from 10 mm to 1 mm [7], [8]. This offering a wide range of features over other frequency bands. These features produce high bandwidth, low interference with current device, frequency reuse, and compact size of the proposed system [9]] [10]. However, one of the key disadvantage of Mm-wave technology is the high path loss, which results in a short range of communicating system. Hence, this technology is mainly proposed for indoor and medium urban environments. For example, the attenuation peak of the Mm-wave channel at several frequencies is investigated in [11].

A high path loss can be seen when the frequency is increased due to the channel loss comes from the atmosphere. At 60 GHz, the attenuation peak is around 15 dB/km at sea level [11]] [12]. The attenuation peak decreases when the frequency is decreased in such way at 26 GHz is about 0.4 dB/km at sea level [13], [14]. Choosing this specific frequency, the path attenuation is significantly reduced by 14 dB at sea level. Hence, this work chooses this center frequency of 26 GHz.

As a point of view less components involving in beamforming design, Nolen matrix is a good candidate due to the excluding of crossover (only coupler and phase shifter are needed). Nevertheless, Nolen matrix with waveguide at Mm-wave band still not yet investigated. However, current

TABLE 2. Related work of nolen matrix.

Ref. No	Properties	Drawbacks
[25]	• 77 GHz frequency of 10 dB • 4 × 4 Nolen matrix • Radar applications	• Insertion loss of 9 dB • Phase error of 8%
[26]	• 3 GHz frequency and isolation of 20 dB • 4 × 4 Nolen matrix • BFNs applications	• Loss in feed line 6dB • Phase error of 6% • BW 400 MHz • gain of 3 dB
[23]	• 5.8 GHz frequency and isolation of 20 dB • 3 × 3 Nolen matrix • BFNs applications	• Narrow BW of 350 MHz • Phase error of 5%
[23]	• 1 GHz frequency and isolation of 10 dB • 3 × 3 Nolen matrix • BFNs applications	• Narrow BW of 70 MHz • Phase error of 10 %
[29]	• 5.8 GHz and isolation of 10 dB • 180 ° coupler • 3 × 3 Nolen matrix • BFNs applications	• Narrow BW of 300 MHz • Phase error of 6 %

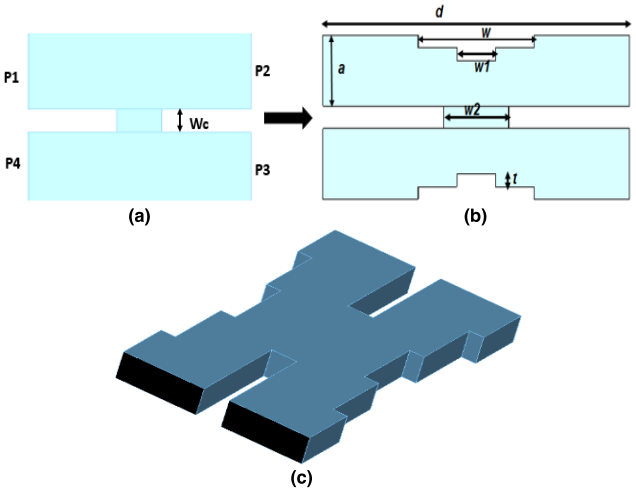

FIGURE 2. Geometry of three couples (a) conventional Structure of waveguide coupler. (b) Proposed coupler. (c) 2D Structure.

studies on Nolen matrix at lower 5G frequency (below 6 GHz) showed an excellent performance relating to low loss and low phase error despite the narrow bandwidth capability [15]. The second problem is related to the antenna design in a matter of providing high gain, high bandwidth and directional beams at Mm-wave band [16], [17]. Waveguide slots antenna is proposed in several studies to provide these requirements [18], [19], [20]. Despite the good gain and directional beams obtained, the antennas have narrow bandwidth due to the use of slots in longitude distribution [21], [22]. Hence, this work focuses to increase the bandwidth by using tilting technique of slot while maintaining a high gain and directive beams.

In this paper, a waveguide-based Nolen matrix with three inputs and three outputs are realized by direct coupling aperture method is presented at 26 GHz. The Nolen matrix

TABLE 3. Dimension of the proposed coupler.

Dim	Definition	Value (mm)
a × b	Inner dim of waveguide	8.636 × 4.318
d	Waveguide length	50
W	Width of narrow wall	19.38
W1	Inner narrow wall	6.46
W2	Coupling area	10.812
t	Thickness of coupling	2.72

TABLE 4. Comparison between simulated and measurement results and other related works at Ka-band.

Parameters	Waveguide Coupler at 26 GHz		Waveguide Coupler at 28 GHz	
	Simulated (dB)	Measured (dB)	Simulated (dB)	Measured (dB)
Return loss (S_{11})	-27	-19	-22	-18
Isolation (S_{41})	-26	-18	-23	-17
Direct (S_{21})	-2.99	-2.77	-3.05	-2.90
Coupling (S_{31})	-3.02	-2.85	-3.12	-3.62
FBW (%)	30	28	30	27
Phase (degree)	90	88.2	89.5	87.2

COMPARISON WITH RELATED WORKS

Ref/year	Freq	BW (GHz)	Output power	Phase error	Loss error
[25]/2017	67 GHz	3	-3.35	4.8°	-7
[26]/2020	26 GHz	1.5	-4.5	15°	-6
[23]/2020	185 GHz	3.5	-5	9°	-9
[29]/2022	28 GHz	0.25	-4.2	3.7°	-10
This Work	26 GHz	7	-3.62, -2.9	2.8°	-5 to -7

components are designed before integrated to form a full 3 × 3 Nolen matrix network. Then, three waveguide slotted antennas are attached to the Nolen matrix outputs. The designed structures are printed using CNC metal printing technology and measured to validate the performance with simulation responses.

II. THEORY OF 3 × 3 NOLEN MATRIX BEAMFORMING NETWORK

The proposed topology of the antenna beamforming using Nolen matrix and waveguide slot antenna is illustrated in figure 1. Typically, 3 × 3 Nolen matrix components are divided into three 3-dB couplers with 90° phase difference at outputs and three phase shifters with 0° and 90°. The most significant part in Nolen matrix design is the 90° coupler design. This is because of the phase difference of the 90° which determines the phase progressions towards the output of the Nolen matrix. A waveguide direct coupling method

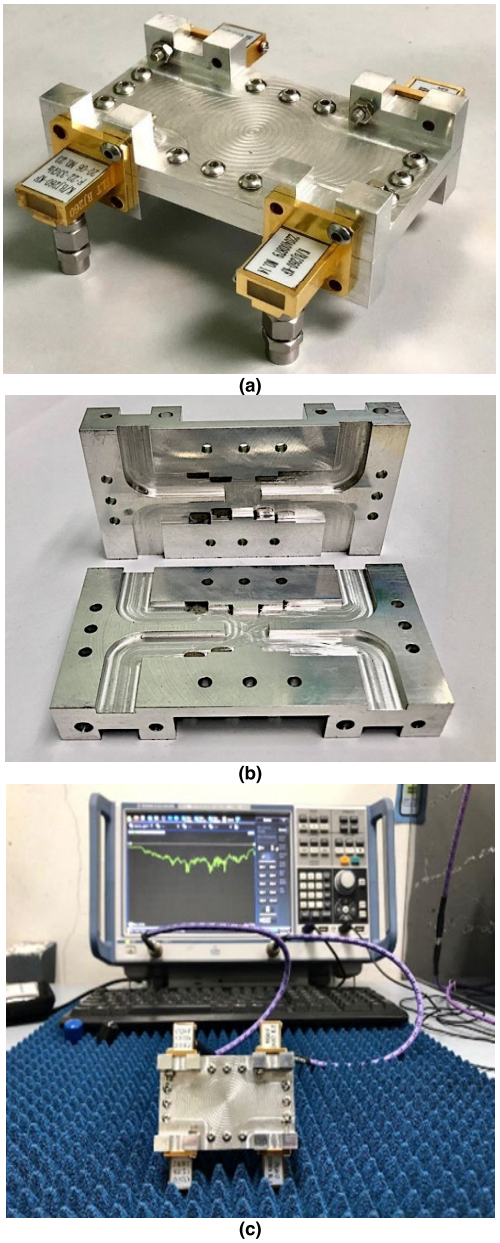

(a)

(b)

(c)

FIGURE 3. Waveguide coupler, (a) fabrication of by using CNC machine, (b) side view of coupler, (c) measure S11 by VNA.

in the narrow wall is chosen to implement the Nolen matrix. Table 1 refer to the Path of input ports into output ports with phase difference.

General form of a Nolen matrix. the conventional Nolen matrix structure consists of couplers and phase shifters without crossover against butler matrix consists from coupler, crossover and phase shifter, the different between BM and Nolen Matrix is crossover. Several studies [21], [22] [23] have been designed Nolen Matrix, some of them have been designed at lower frequency with couplers and phase shifters based on specific integration to achieved correct phase different at output ports. In additional Nolen Matrix has flexibly of input and output ports. Fig 1 refers to the configuration

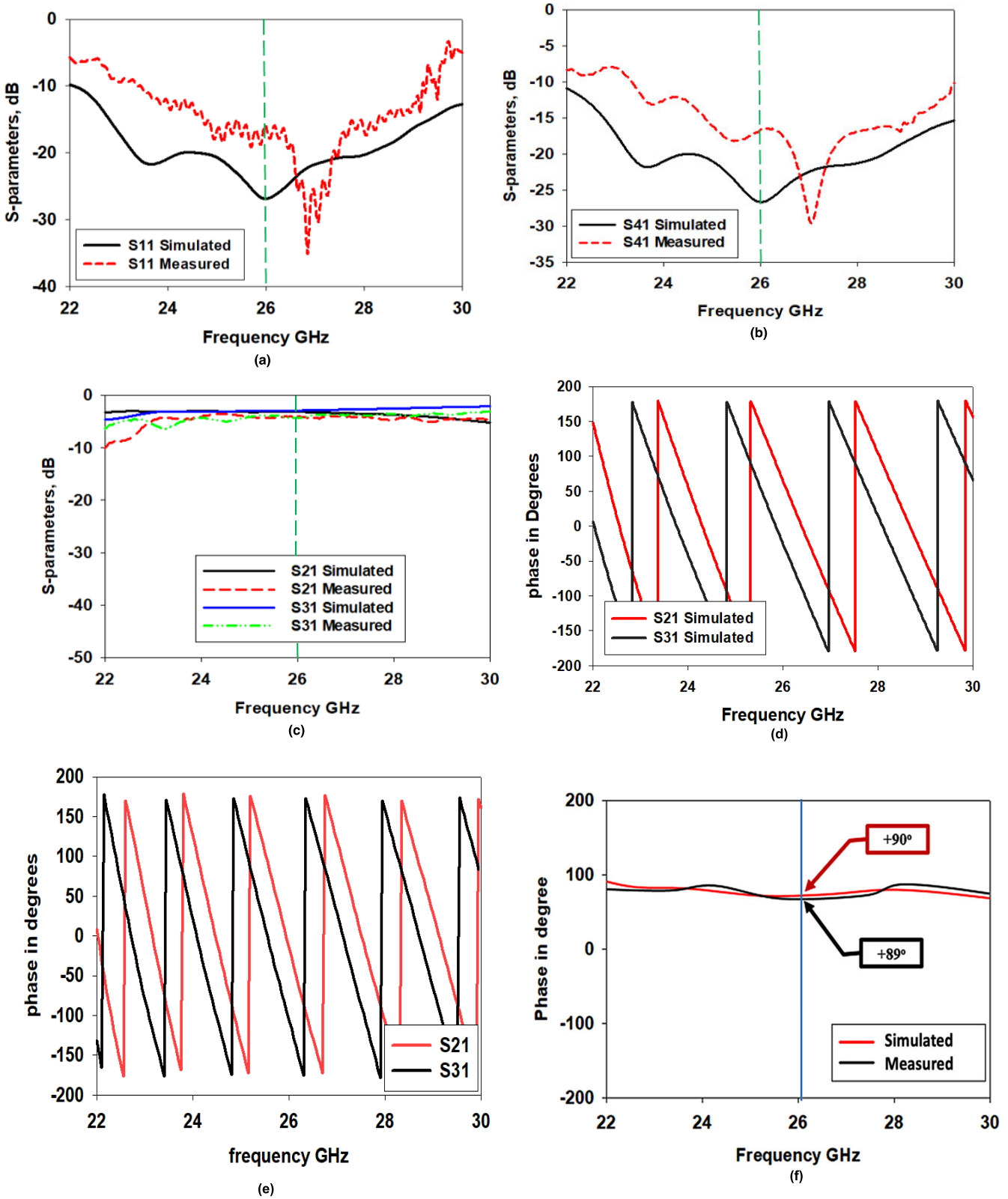

FIGURE 4. Coupler performance. (a, b, c) S-parameters, (d) simulation Phase, (e) measure phase, (f) simulation and measurement difference at outputs.

and integration way of Nolen Matrix components between each other's to achieved good performance. Three couplers and one phase shifter only have been used in this paper to build 3 × 3 Nolen Matrix.

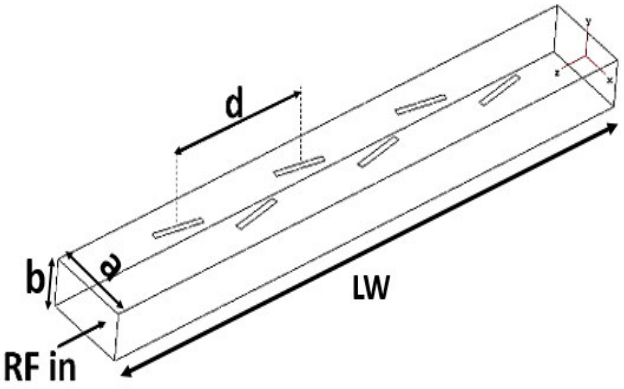

(a)

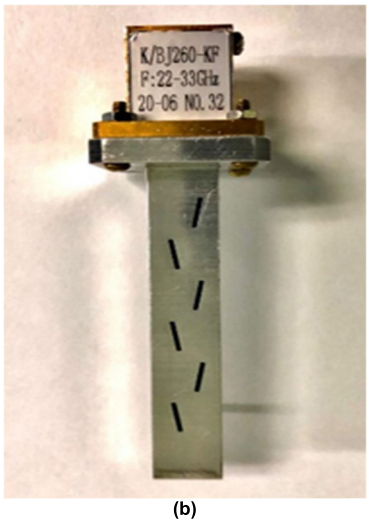

(b)

FIGURE 5. Waveguide tilt slots antenna, (a) simulation, (b) fabrication.

TABLE 5. A dimensions of the proposed antenna.

Parameters	describe	Value
a	Broad wall	0.75 λ
b	Narrow wall	0.35 λ
LW	Length of waveguide	5.2 λ
L	Length of slot	0.46 λ
d	distance between slots	0.63 λ
W	Width of slot	0.052 λ
θ	Angle of slots	±10 degree

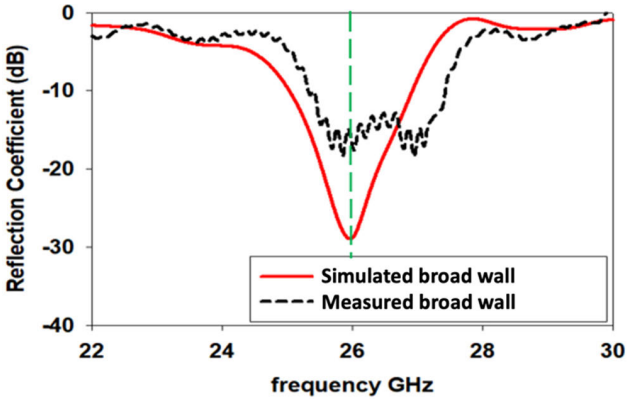

(a)

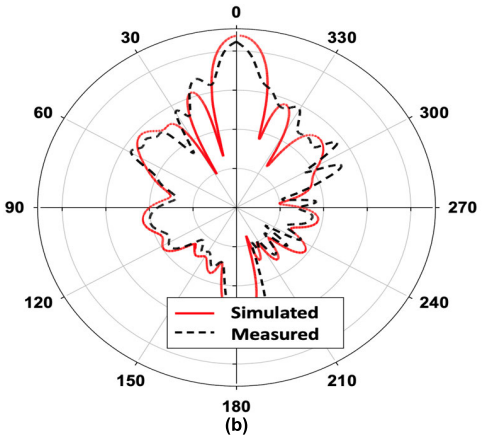

(b)

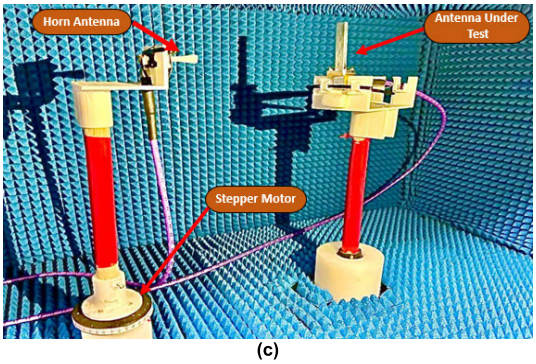

(c)

FIGURE 6. Performance of the proposed antenna. (a) S-parameters. (b) Radiation pattern comparisons. (c) test antenna in chamber room.

At different coupling ratio of the coupling with different phase difference, the Nolen matrix phase difference at outputs can be calculated as follows [23].

$$at\ P1 : (\angle S_{51} - \angle S_{41}) - (\angle S_{61} - \angle S_{51}) \quad (1)$$

$$at\ P2 : (\angle S_{52} - \angle S_{42}) - (\angle S_{62} - \angle S_{52}) \quad (2)$$

$$at\ P3 : (\angle S_{53} - \angle S_{43}) - (\angle S_{63} - \angle S_{53}) \quad (3)$$

$$\angle S_{41} = 90^\circ \quad (4)$$

$$\angle S_{51} = 90^\circ - \theta_1 + 90^\circ \quad (5)$$

$$\angle S_{61} = 90^\circ - \theta_1 + 90^\circ \quad (6)$$

$$\angle S_{42} = 90^\circ - \theta_1 + 90^\circ \quad (7)$$

$$\angle S_{52} = \tan^{-1}\left(\frac{Im\left(e^{j(90^\circ-2\theta_1)} + \sqrt{3}e^{j(180^\circ-\theta_2)}\right)}{Re\left(e^{j(90^\circ-2\theta_1)} + \sqrt{3}e^{j(180^\circ-\theta_2)}\right)}\right) \quad (8)$$

$$\angle S_{62} = \tan^{-1}\left(\frac{Im\left(e^{j(90^\circ-2\theta_1)} + \sqrt{3}e^{j(-\theta_2)}\right)}{Re\left(e^{j(90^\circ-2\theta_1)} + \sqrt{3}e^{j(-\theta_2)}\right)}\right) \quad (9)$$

$$\angle S_{43} = 90^\circ - \theta_1 + 90^\circ \quad (10)$$

$$\angle S_{53} = \tan^{-1}\left(\frac{Im\left(e^{j(90^\circ-2\theta_1)} + \sqrt{3}e^{j(-\theta_2)}\right)}{Re\left(e^{j(90^\circ-2\theta_1)} + \sqrt{3}e^{j(-\theta_2)}\right)}\right) \quad (11)$$

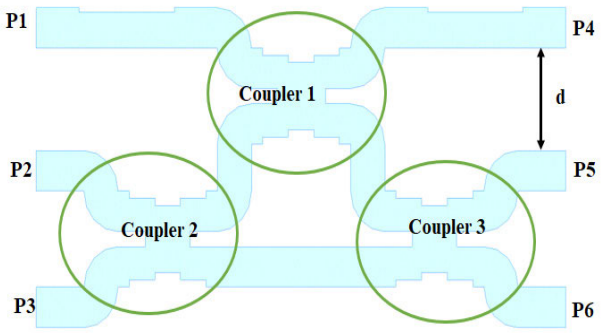

FIGURE 7. The integration of three couplers to build 3 × 3 Nolen matrix.

$$\angle S_{63} = \tan^{-1}\left(\frac{Im\left(e^{j(90^\circ-2\theta_1)} + \sqrt{3}e^{j(-180^\circ-\theta_2)}\right)}{Re\left(e^{j(90^\circ-2\theta_1)} + \sqrt{3}e^{j(-180^\circ-\theta_2)}\right)}\right) \quad (12)$$

The values of the phase shifters are found by substituting (1) - (3) into (4) - (7). Hence, $\theta_1 = 90^\circ$ and $\theta_2 = 90^\circ$, which reduces the phase shifters number in the Nolen matrix. Therefore, after determination of coupling ratio and phase shifter values, the output powers of Nolen matrix should be equally divided into −6 dB at each port (P4, P5, and P6). The phase different of the Nolen matrix based on input ports has the value of 0°, 150°, and −90° at port 1, port 2, and port 3 respectively. The topology of the waveguide coupler is illustrated in figure 2. The waveguide coupler is a type of two-branch of λ/4 wavelength transmission lines. A rectangular waveguide structure technique is chosen to design the proposed coupler. Thus, the two-branch lines (in figure 2 (a)) can be represented with coupling aperture and cutting in narrow wall as shown in figure 2 (b). Table 2 presented the related work of waveguide Nolen matrix at higher frequency.

III. COUPLER

Coupler is a passive component that is prominently utilized for power division in beamforming network. The conventional 3 dB couplers such as quadrature (branch-line) hybrid, directional and Lange couplers will receive an input signal from an input port and divide the signals between two output ports for power division. For instance, the 3 dB quadrature hybrid coupler has similar power split ratio but the phase between output ports (port 2 and port 3) of the couplers differs in 90° [25]. The symmetry branch-line coupler is reflected in the scattering matrix whereby each row can be determined as a transposition of the first row. The scattering matrix, [S] can be defined as Equation 4 [25], [26], [27], [28]. As a results, the final dimension of the proposed coupler is obtained from the above parametric study and summarized in Table 3. Figure 2 (c) illustrates the final design of the coupler with the simulation results. The designed coupler in figure 3 (a) shows fabrication design with arms of input and output port of the proposed design, this is due to the very small distance between the input and output ports which

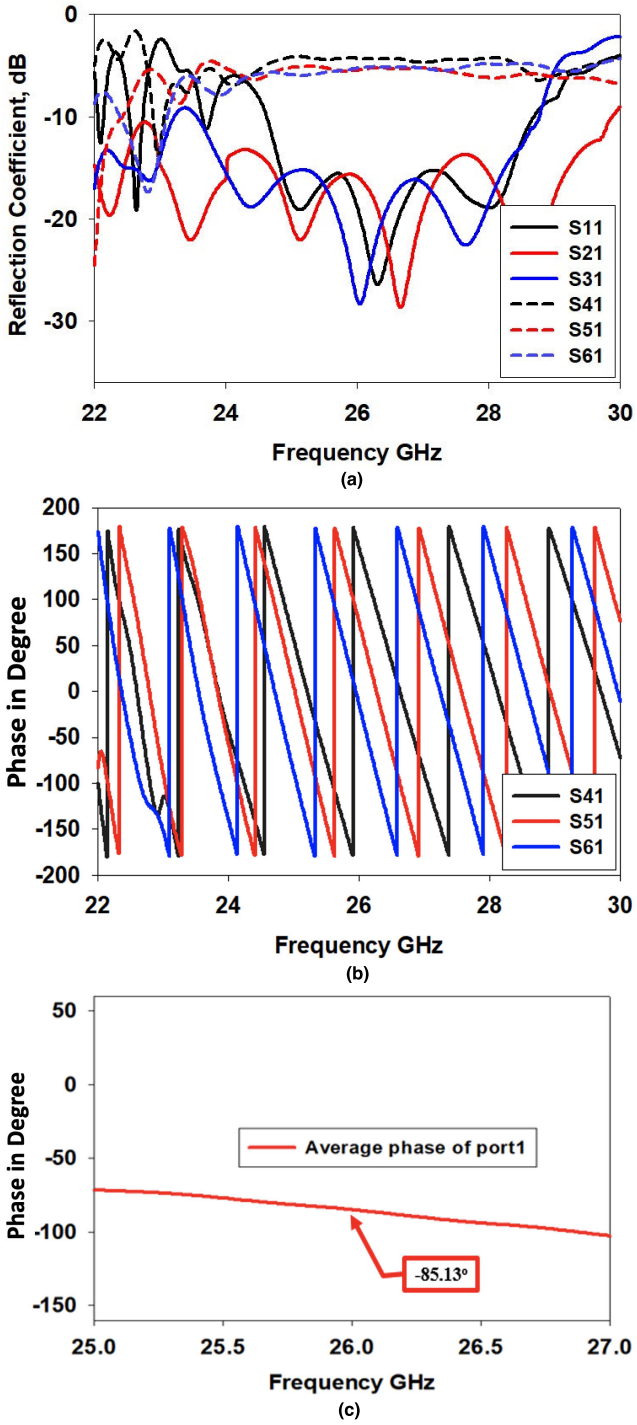

FIGURE 8. Simulated response of Nolen matrix at port 1. (a) S-parameters. (b) Phases at outputs. (c) Phase difference at outputs.

makes measurement using arms to separate each adjacent port. The reflection coefficient S_{11} is −35 dB, which means a good return loss is obtained with higher bandwidth of more than 10 GHz. Figure 3(b) refer to the two half pieces with smooth surface of coupler have been fabricated by using CNC machine. Figure 3 (c) refer to the waveguide coupler during measure the reflection coefficient by VNA in UTM chamber.

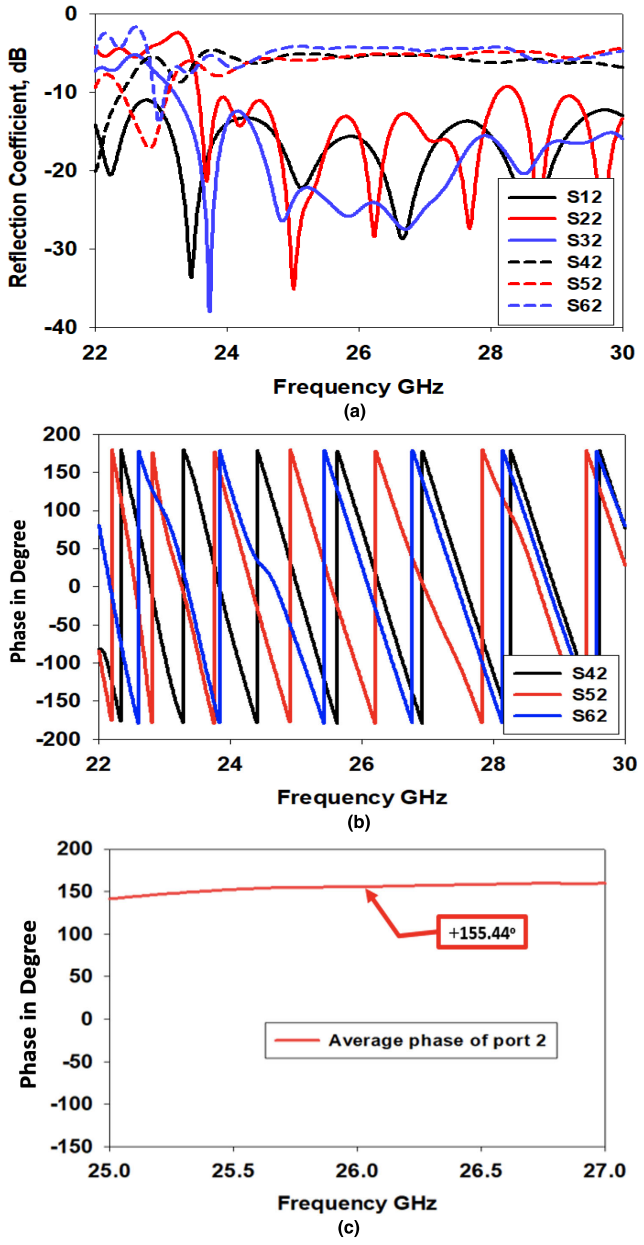

FIGURE 9. Simulated response of Nolen matrix at port 2. (a) S-parameters. (b) Phases at outputs. (c) Phase difference at outputs.

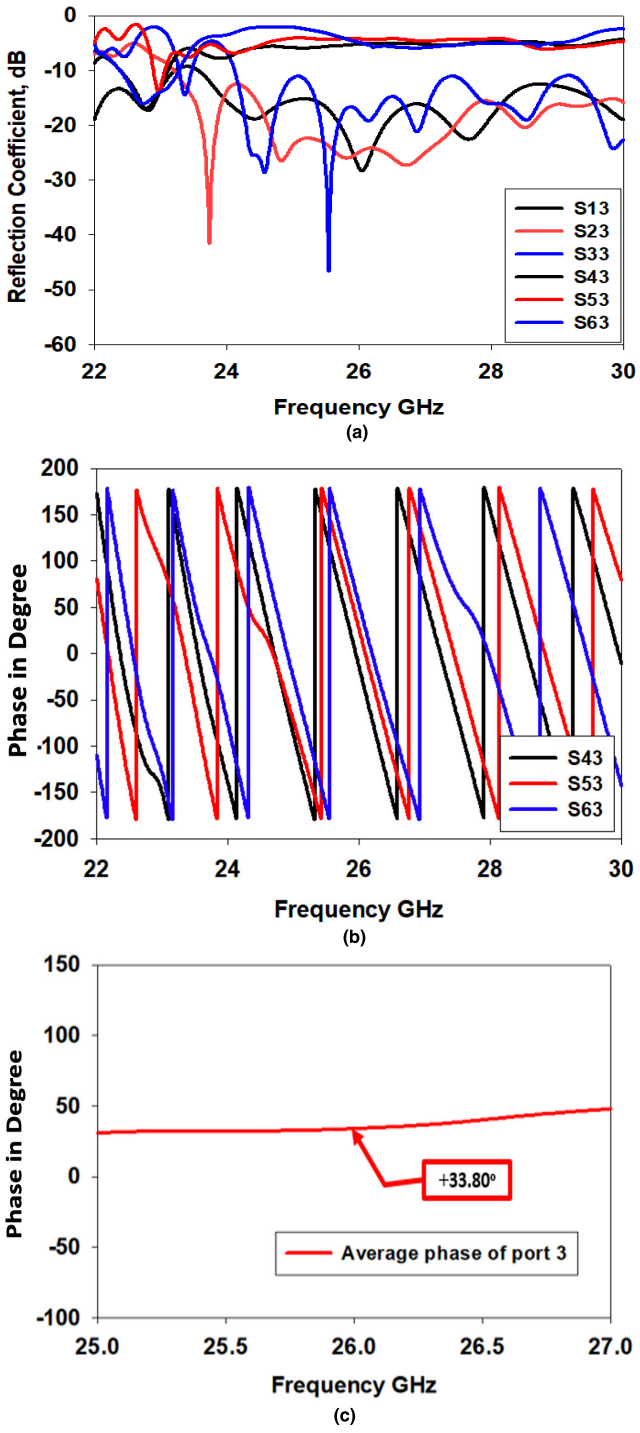

FIGURE 10. Simulated response of Nolen matrix at port 3. (a) S-parameters. (b) Phases at outputs. (c) Phase difference at outputs.

Two coaxial cables have been integrated with adapter of waveguide port and two terminate load have been used on the reset of ports to measure waveguide coupler.

The coupling matrix and the phases calculated from (1) to (12) of the waveguide coupler are obtained at 26 GHz, the proposed 90° coupler structure with coupling aperture is determined. The simulation result of the proposed coupler is shown in figure 4 (a, b, c). The return loss summation, S11 = −27 dB with measured S11 = −19, which means a good return loss is obtained. The power is evenly divided between port 2 and 3 with S21 = −3.12 dB and S31 = −3.08 dB which indicates a successfully split power of 3 dB between the output ports. The isolation is less than −10 dB.

Figure 4(d) refer to the simulation phase of port 1, while Figure 4(e) refer to the measure phase of port 1. figure 4(f) refer to the comparation phase difference at outports, the proposed waveguide coupler achieved 90° phase difference at output ports as simulation results, while achieved 89 phase difference as measure results. Hence, the phase error is 1° within the desired 90° phase. A comparison between the

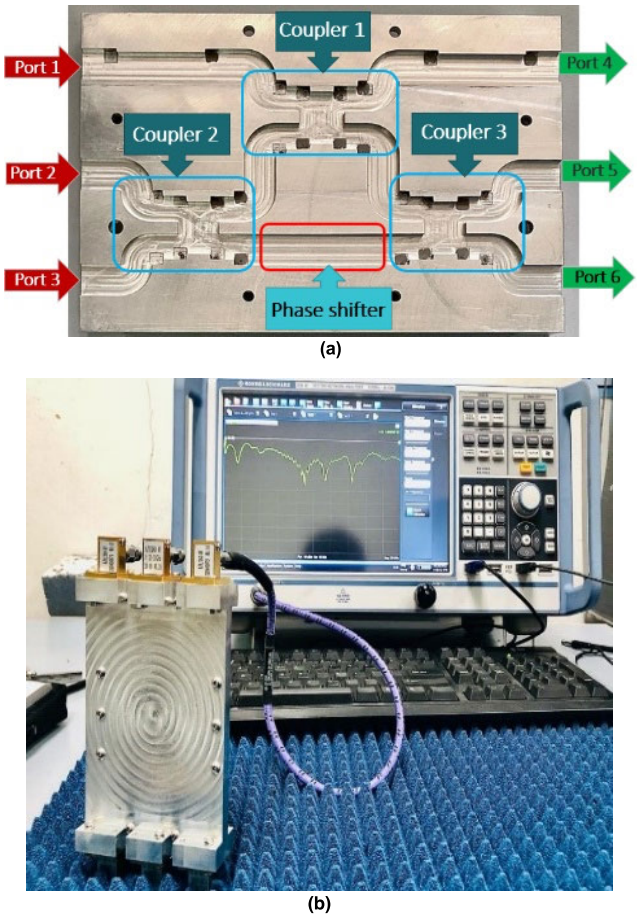

FIGURE 11. Fabricated response of the propose antenna beamforming at 26 GHz. (a) proposed beamforming by using CNC machine, (b) Return loss.

printed Coupler with previously published works are presented in Table 4. Hence, the proposed Coupler shows low loss priorities and ultra-wideband, in which benefits the main requirements for 5G systems and applications at millimeter wave.

IV. DESIGN WAVEGUIDE ANTENNA

Rectangular waveguide WR34 antenna is selected to distribute slots. As shown in figure 5(a) simulation design of waveguide tilt antenna, the slot is spread on a broad wall with a tilt angle (θ) that is spun around the slot's center. The slots are cut symmetrically into the broad walls of the waveguide by the transverse current when the mode is TE_{10}. As a result, Table 5 summarizes the intended antenna size in lambda. Figure 5 (b) shows the fabrication design of the proposed design by using CNC machine. Figure 6 (a) the simulation and measured return loss, S_{11} of the waveguide slots tilt antenna . The measured radiation pattern is shown in figure 6 (b), representing the directional beam of the waveguide slots tilt antenna. Figure 6 (c) refer to the test antenna in camber room.

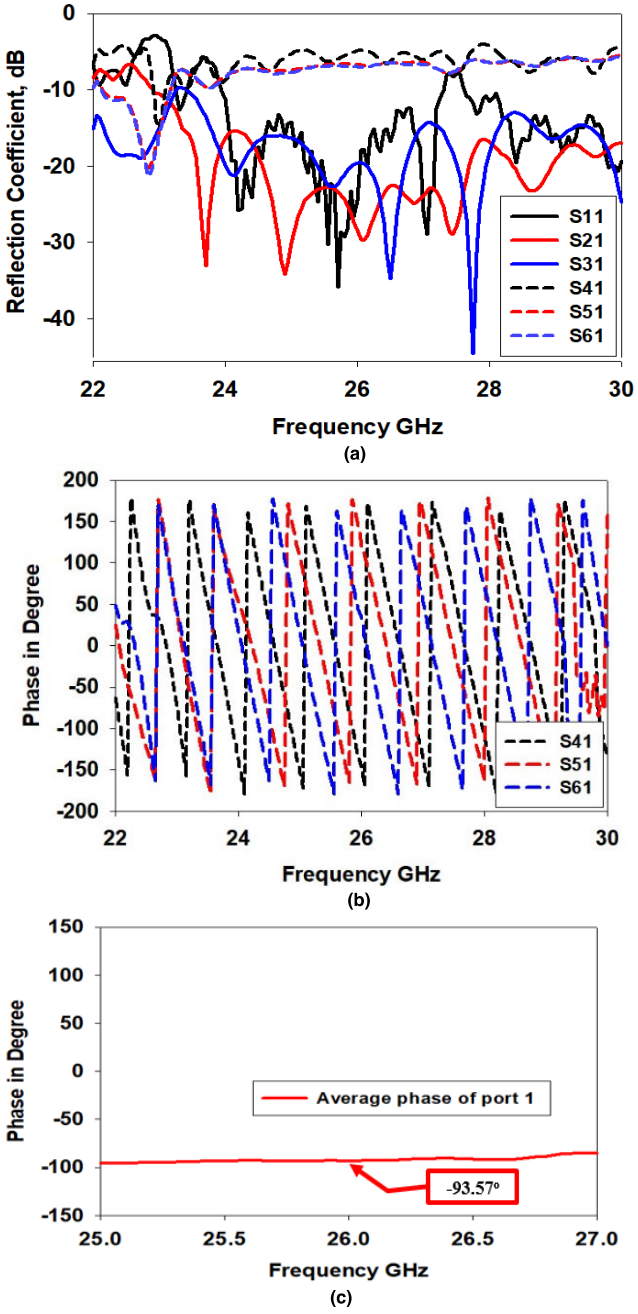

FIGURE 12. Performance of the proposed 3 × 3 Nolen matrix. (a) S-parameters, (b) Phase difference at port 1.

V. BUILD NOLEN MATRIX BY INTEGRATION OF THREE COUPLERS

The designed coupler which previously discuses is integrated together to form the Nolen matrix beamforming circuit as shown in figure 7. In order to optimize the proposed Nolen circuit, a 90° E-bends waveguide are added to the Nolen matrix input and the output ports. The radius of these four 90° E-bends waveguide are chosen to be 15.17 mm to prevent any reflections from these bends. The initial distance d is λ/2

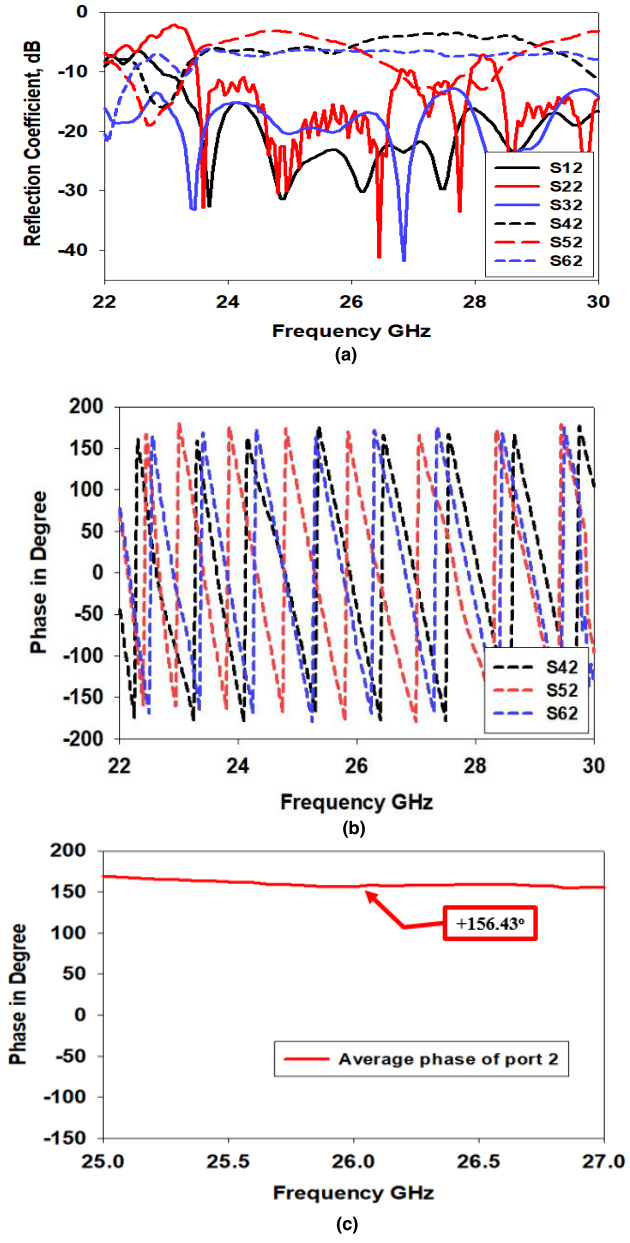

FIGURE 13. Performance of the proposed 3 × 3 Nolen matrix. (a) S-parameters, (b) Phase difference at port 2.

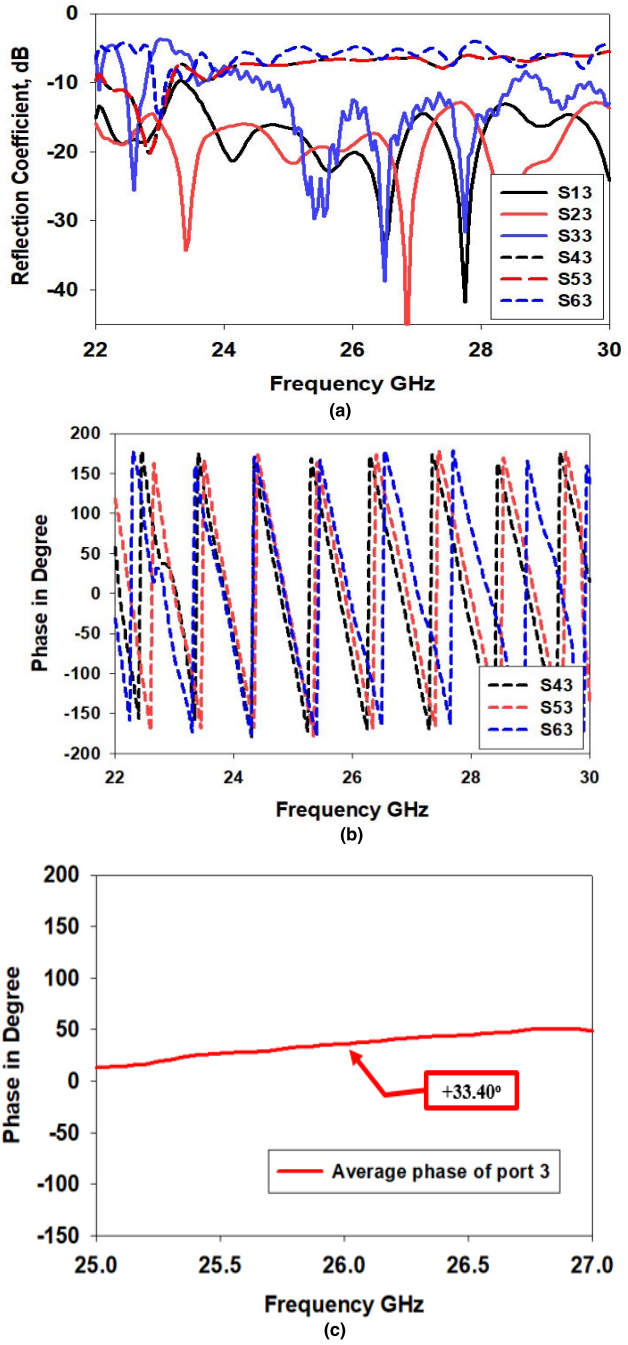

FIGURE 14. Performance of the proposed 3 × 3 Nolen matrix. (a) S-parameters, (b) Phase difference at port 3.

(5.35 mm) between input/output ports. However, to maintain enough space between the antenna elements, the optimized distance d is fixed to 18 mm.

The simulated performance of the proposed Nolen is plotted in figure 8, figure 9, and figure 10 at each port 1, port 2, and port 3 are excited. Figure 8 (a) shows the return loss, isolation, and insertion loss results when port 1 is excited. All the values are agreed well with the concepts of operation of the Nolen matrix. At 26 GHz, a return loss and isolation are below −10 dB with insertion loss of −6.5 dB at outputs. Figure 8 (b) and figure 8 (c) illustrate the phase and average phase difference responses at the outputs which is −90 degree. Figure 9 (a) shows the return loss, isolation, and insertion loss results when port 2 is excited. All the values are agreed well with the concepts of operation of the Nolen matrix. At 26 GHz, a return loss and isolation are below −10 dB with insertion loss of 7 dB at outputs. Figure 9 (b) and figure 9 (c) illustrate the phase and average phase difference responses at the outputs which is +150 degree. Figure 10 (a) shows the return loss, isolation, and insertion loss results when port 3 is excited. All the values are agreed well with the concepts of operation of the Nolen matrix. At 26 GHz,

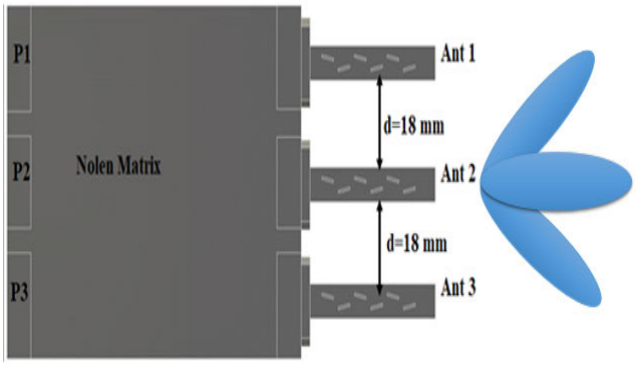

FIGURE 15. The proposed beamforming network with three waveguide tilt slot antennas array.

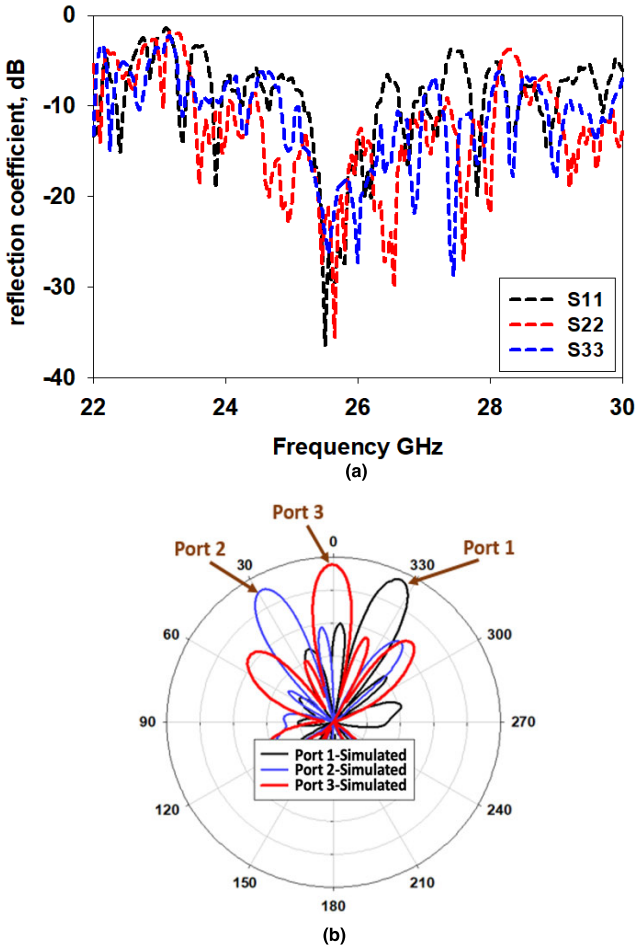

FIGURE 16. Simulated response of the propose antenna beamforming at 26 GHz. (a) Return loss of the inputs. (b) Radiation patterns.

a return loss and isolation are below −10 dB with insertion loss of −6.8 dB at outputs. Figure 10 (b) and figure 10 (c) illustrate the phase and average phase difference responses at the outputs which is +30 degree.

VI. FABRICATION AND MEASUREMENT OF WAVEGUIDE NOLEN MATRIX

Figure 11 (a) presented half view of 3 × 3 Nolen matrix printed using CNC machine. The performance of prototypes

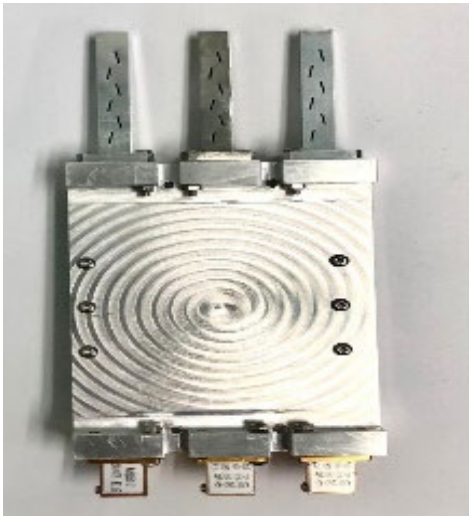

FIGURE 17. Nolen matric beamforming.

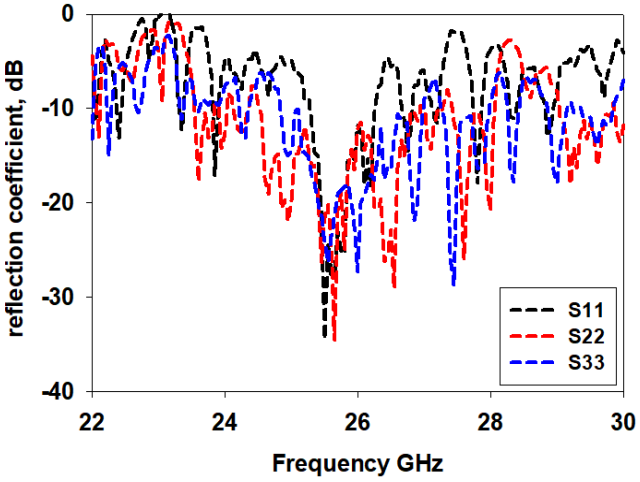

FIGURE 18. The measurment reutren loss of Nolen matrix beamforming.

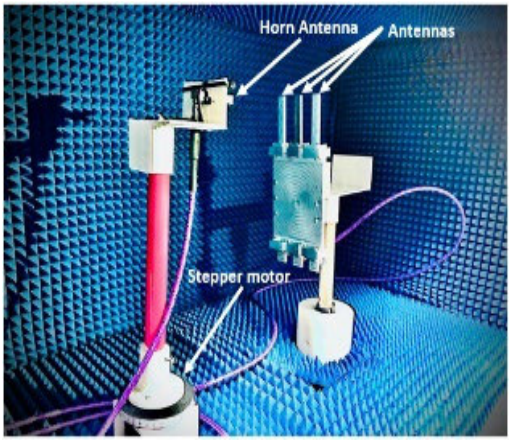

FIGURE 19. Nolen matrix beamforming in chamber room.

is validated using two ports R&S®ZNB40 VNA. A WR-34 waveguide-coaxial adaptor is used with termination loads are placed at the other ports during the measurements. Return loss

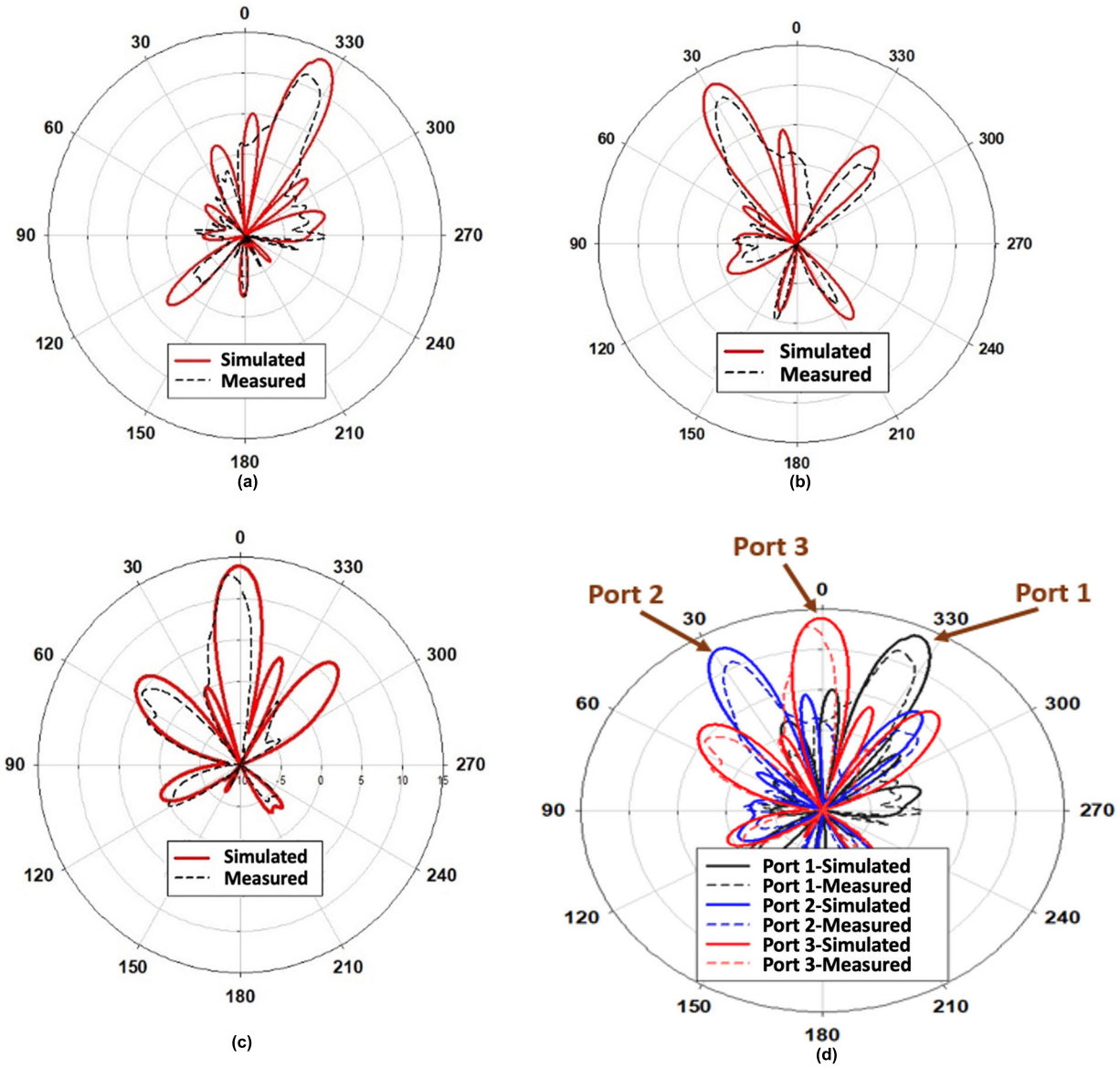

FIGURE 20. Measurement and simulation radiation of the proposed antenna beamforming network. (a) port1. (b) port2, (c) port3, (d) comparison radiation pattern of Nolen matrix beamforming.

of fabrication response of the propose Nolen matrix at 26 GHz has been measured by VNA as show in figure 11(b).

The measured S-parameters results are plotted in figure 12 (a), as port 1 is excited. The measured return loss is −25.02dB, and insertion loss is −5dB. The measured phase differences present in figure 12(b), was (S51-S41), (S61, S51), −93.3° and −94°, is achieved between output ports P-4/P-5 and P-5 / P-6, respectively, when the signal is fed to Port-1. It is important to note here that from the measured phase difference values, the error is 3.3° and 4°, respectively. The average phase difference was −93.57° and error of average is 3.57°. as can see in figure 12(c).

The measured S-parameters results of port 2 are plotted in figure 13 (a), The measured of return loss is −27.02dB and insertion loss is −5.6 dB. The measured phase differences present in figure 13(b), was (S51-S41), (S61, S51), 158.53° and 154.36°, is achieved between output ports P-4/P-5 and P-5 / P-6, respectively, when the signal is fed to Port-2. It is important to note here that from the measured phase difference values, the error is 8.5° and 4.3°, respectively. The average phase difference was +156.43° and error of average is 6.43°. as can see in figure 13(c).

The measured S-parameters results of port 3 are plotted in figure 14 (a), The measured of return loss is −28 dB and insertion loss is −6.6 dB. The measured phase differences present in figure 14(b), was (S51-S41), (S61, S51), 31.6° and 35.2°, is achieved between output ports P-4/P-5 and P-5 / P-6, respectively, when the signal is fed to Port-3. It is important to note here that from the measured phase difference values, the error is 5.2° and 1.6°, respectively. The average phase difference was +33.40° and error of average is 3.4°. as can see in figure 14(c).

VII. INTEGRATION OF ANTENNA WITH NOLEN MATRIX

Then, the proposed Nolen matrix network is attached with three antennas array as shown in figure 15. The antennas are connected to the output ports through the WR-34 flange standard. The antennas are designed and validated to form directive beam and the performance can be found in [16]. The distance d is fixed to 18 mm, which is maintaining an enough space between the antenna elements due to the use of the WR-34 flange standard.

The simulated results of the proposed antenna beamforming are plotted in figure 16. The return loss at all ports is less than −10 dB at 26 GHz with a bandwidth of 4 GHz as shown in figure 16 (a). The responses of the three beams radiation patterns are shown in figure 16 (b). At port 1 the beam is located at −30° with gain of 14.5dB. At port 2 the beam is located at +30° with gain of 14.8dB. The beam at port 3 is located at 0° with gain of 14.5dB. All the beam scanning is ranging between ±30°. Hence, the output phases are correctly assigned the three beams from the proposed Nolen matrix.

VIII. ANTENNA BEAMFORMING NETWORK RESULTS

Figure 17 refer to the proposed waveguide beamforming Nolen matrix has been fabricated by using CNC machine and waveguide antenna has been integrated with Nolen matrix by using flange.

The measured return loss, S_{11} and S_{22} = 23.78 dB, and the measured return loss S_{33} = 14.32 as can see in figure 18, which means a good return loss is obtained at 26 GHz, despite the losses due to the fabrication tolerance. The proposed design achieved bandwidth 3GHz at resonate frequency 26Ghz.

The radiation pattern measurement which done in the Anechoic Chamber of Advanced Microwave and RF Antenna Lab, Universiti Teknologi Malaysia (UTM), Johor, Malaysia. The tested antennas placed towards the source antenna as shown in Figure 19.

Figure 20 (a-b-c) shows the simulated and measured results of the radiation pattern of linear 1 × 3 antenna array with a spacing of 0.5λ, when Port-1, Port-2 and Port-3 of the BFN are excited. The simulation results were already discussed in the previous section, so now onwards, the discussion is related to the measured results. When Ports-1 or 3 were excited, a gain of 14.21 dB and 14.38 dB was achieved, respectively. Meanwhile, the gain was 12.47 dB at port 2 excitation, respectively. However, according to which input was excited, the peak of the beam rotates. When Port-1 was fed with a signal, the main beam steered to −11.47°. Meanwhile, the direction of radiation was attained at −27°, as the signal was fed into Port-2, for the Port-3 excitation, the main beam steers to +28. Figure 20 (d) show Simulated and measured radiation patterns of the multi beam antenna array.

The scanning angles of −26° and −6° were obtained at port 1 and port 3 respectively and port 2 scanning angle at +27° as shown in Table 6. Table 7 compares the performance of the proposed antenna beamforming prototype with other related designs. It can be concluded from the comparison that the prototype has a low phase error of 3° and better scanning angle error and losses of ±5° and 5 dB respectively.

TABLE 6. Comparison of the simulated and measured for beam-scanning.

Number of port	Perfect phase	Simulation		Measurement	
		Average phase	Phase error	Average phase	Phase error
1	-30	-27	3	-26	4
2	+30	+28	4	+27	3
3	0	3	3	+6	6

TABLE 7. Comparison with related works.

Parameters	[30]	[31]	[20]	[31]	This work
Frequency (GHz)	28	28	20	28	Ka-band
Return loss (dB)	30	15.6	23.2	20.54	23
Isolation (dB)	25	25.5	20.12	23.12	25
Bandwidth (GHz)	3	0.85	1	0.65	3
Insertion loss (dB)	9.8	10	9	6 to 7	6.7
Phase errors (degree)	11	9	6	3	±5°
Losses (dB)	8	10	7.5	5	5
Scanning angle (degree)	±12, ±51	±35, ±10	±40	±20, ±42	-26°, +27°, 0°
Gain (dB)	12	24	18	15.21	14.38
Technology	SIW	Waveguide	Waveguide	Cavity resonator	Waveguide

IX. CONCLUSION

A fully waveguide based Nolen matrix beamforming network with waveguide slotted antenna array has been presented in this paper. The designed components and Nolen matrix network based on direct coupling have been discussed. A three waveguide tilts slots antennas are attached to the outputs of the proposed 3 × 3 Nolen matrix. There are two available techniques to fabricate the proposed design, first is 3D printing, this technique is not really suitable to fabricate structure because 3D printing leaves mesh inside waveguide also the weight of design been heavy and high cost. CNC has been using to fabricate design because low cost, not heavy and create smooth hollo waveguide, CNC fabricated half of design two times and then integrated together to achieved full shape of design. The structure has been fabricated using CNC printing technology. The performance of the printed beamforming network showed an excellent agreement with the simulated responses. A good reflection and isolation are obtained with less than −10 dB at 26 GHz. A directive Beas with maximum gain of 14.38 dB is obtained at scanning angle between −27° to +28°. Overall, the waveguide Nolen matrix beamforming network shows good performance and has great potential for millimeter wave applications.

REFERENCES

[1] T. Wang and B. Huang, "Millimeter-wave techniques for 5G mobile communications systems: Challenges, framework and way forward," in *Proc. 31st URSI Gen. Assem. Sci. Symp. (URSI GASS)*, Beijing, China, Aug. 2014, pp. 1–4, doi: 10.1109/URSIGASS.2014.6929247.

[2] Y. M. Hussein, M. K. A. Rahim, N. A. Murad, and H. O. Hanoosh, "Low loss wideband 4 × 4 Butler matrix networks based on substrate integrated waveguide for 5G applications," *IEEE Access*, vol. 12, pp. 7896–7910, 2024, doi: 10.1109/ACCESS.2023.3342713.

[3] W. Roh, J.-Y. Seol, J. Park, B. Lee, J. Lee, Y. Kim, J. Cho, K. Cheun, and F. Aryanfar, "Millimeter-wave beamforming as an enabling technology for 5G cellular communications: Theoretical feasibility and prototype results," *IEEE Commun. Mag.*, vol. 52, no. 2, pp. 106–113, Feb. 2014, doi: 10.1109/MCOM.2014.6736750.

[4] K. K. Naidu and S. I. Rosaline, "Beamforming networks for 5G. A literature review of Butler matrix," in *Proc. Int. Conf. Electron., Comput., Commun. Control Technol. (ICECCC)*, Bengaluru, India, May 2024, pp. 1–10, doi: 10.1109/iceccc61767.2024.10593844.

[5] S.-G. Mok, C.-W. Jung, S.-J. Ha, and Y. Kim, "Switchable beam pattern antenna for wireless communication devices," in *Proc. IEEE Int. Symp. Antennas Propag. (APSURSI)*, Spokane, WA, USA, Jul. 2011, pp. 1308–1310, doi: 10.1109/APS.2011.5996529.

[6] M. A. Saeed and A. O. Nwajana, "A review of beamforming microstrip patch antenna array for future 5G/6G networks," *Frontiers Mech. Eng.*, vol. 9, Feb. 2024, Art. no. 1288171, doi: 10.3389/fmech.2023.1288171.

[7] Y. J. Cheng, W. Hong, K. Wu, Z. Q. Kuai, C. Yu, J. X. Chen, J. Y. Zhou, and H. J. Tang, "Substrate integrated waveguide (SIW) Rotman lens and its Ka-band multibeam array antenna applications," *IEEE Trans. Antennas Propag.*, vol. 56, no. 8, pp. 2504–2513, Aug. 2008, doi: 10.1109/TAP.2008.927567.

[8] T. Empliouk, P. Kapetanidis, D. Arnaoutoglou, C. Kolitsidas, D. Lialios, A. Koutinos, T. N. F. Kaifas, S. V. Georgakopoulos, C. L. Zekios, and G. A. Kyriacou, "Compact, ultra-wideband Butler matrix beamformers for the advanced 5G band FR3—Part I," *Electronics*, vol. 13, p. 2763, Jun. 2024.

[9] F. Casini, R. V. Gatti, L. Marcaccioli, and R. Sorrentino, "A novel design method for Blass matrix beam-forming networks," in *Proc. Eur. Radar Conf.*, Munich, Germany, Oct. 2007, pp. 232–235, doi: 10.1109/eurad.2007.4404979.

[10] Y. E. Yamaç, A. Çalişkan, A. S. Türk, and A. Kızılay, "A low-profile hollow waveguide slot array antenna with full-corporate feeding network at K-band," *Adv. Electromagn.*, vol. 11, no. 2, pp. 23–27, May 2022, doi: 10.7716/aem.v11i2.1829.

[11] E. F. Nymphas and O. Ibe, "Attenuation of millimetre wave radio signal at worst hour rainfall rate in a tropical region: A case study, Nigeria," *Sci. Afr.*, vol. 16, Jul. 2022, Art. no. e01158, doi: 10.1016/j.sciaf.2022.e01158.

[12] M.-A. Chung, C.-W. Lin, and C.-W. Yang, "A low-cost four-directional beamforming switched Butler matrix network antenna for 5G NR applications," *IEEE Access*, vol. 12, pp. 42949–42960, 2024, doi: 10.1109/ACCESS.2024.3379235.

[13] A. Giannini, M. Mercolino, A. Graziani, and A. Martellucci, "Preliminary analysis of atmospheric attenuation and sky brightness temperature at deep-space antenna site of Cebreros for communications in Ka band," in *Proc. 11th Eur. Conf. Antennas Propag. (EUCAP)*, Paris, France, Mar. 2017, pp. 40–44, doi: 10.23919/EuCAP.2017.7928735.

[14] E. M. Mohamed, A. Mchbal, A. Marroun, and N. A. Touhami, "Antenna feeding network design for 5G massive MIMO applications," in *Proc. Int. Conf. Global Aeronaut. Eng. Satell. Technol. (GAST)*, Marrakesh, Morocco, Apr. 2024, pp. 1–5, doi: 10.1109/gast60528.2024.10520807.

[15] W. Choi, K. Park, Y. Kim, K. Kim, and Y. Kwon, "A *V*-band switched beam-forming antenna module using absorptive switch integrated with 4 × 4 Butler matrix in 0.13-μm CMOS," *IEEE Trans. Microw. Theory Techn.*, vol. 58, no. 12, pp. 4052–4059, Dec. 2010, doi: 10.1109/TMTT.2010.2086472.

[16] S. A. Babale, S. K. A. Rahim, O. A. Barro, M. Himdi, and M. Khalily, "Single layered 4 × 4 Butler matrix without phase-shifters and crossovers," *IEEE Access*, vol. 6, pp. 77289–77298, 2018, doi: 10.1109/ACCESS.2018.2881605.

[17] G. Zhang, H. Yan, P. Liu, S. Z. Pour, and B. Arigong, "High-capacity multiple-input multiple-output communication for Internet-of-Things applications using 3D steering Nolen beamforming array," *Electronics*, vol. 13, no. 13, p. 2452, 2024, doi: 10.3390/electronics13132452.

[18] W. M. Dyab, A. A. Sakr, and K. Wu, "Dually-polarized Butler matrix for base stations with polarization diversity," *IEEE Trans. Microw. Theory Techn.*, vol. 66, no. 12, pp. 5543–5553, Dec. 2018.

[19] M. F. Hagag, R. Zhang, and D. Peroulis, "High-performance tunable narrowband SIW cavity-based quadrature hybrid coupler," *IEEE Microw. Wireless Compon. Lett.*, vol. 29, no. 1, pp. 41–43, Jan. 2019.

[20] T. Tomura, D.-H. Kim, M. Wakasa, Y. Sunaguchi, J. Hirokawa, and K. Nishimori, "A 20-GHz-band 64 × 64 hollow waveguide two-dimensional Butler matrix," *IEEE Access*, vol. 7, pp. 164080–164088, 2019.

[21] P. Li, H. Ren, and B. Arigong, "A symmetric beam-phased array fed by a Nolen matrix using 180° couplers," *IEEE Microw. Wireless Compon. Lett.*, vol. 30, no. 4, pp. 387–390, Apr. 2020, doi: 10.1109/LMWC.2020.2972728.

[22] M. A. Tulum, A. S. Turk, and P. Mahouti, "Data driven surrogate modeling of phase array antennas using deep learning for millimetric band applications," *IEEE Access*, vol. 11, pp. 114415–114423, 2023, doi: 10.1109/access.2023.3324733.

[23] H. Ren, H. Zhang, and B. Arigong, "Ultra-compact 3 × 3 Nolen matrix beamforming network," *IET Microw., Antennas Propag.*, vol. 14, no. 3, pp. 143–148, 2020, doi: 10.1049/iet-map.2019.0336.

[24] M. A. Fuentes-Pascual, M. Baquero-Escudero, M. Ferrando-Rocher, J. I. Herranz-Herruzo, and A. Valero-Nogueira, "5 × 7 Nolen matrix in K-band implemented in rectangular waveguide," in *Proc. 18th Eur. Conf. Antennas Propag. (EuCAP)*, Glasgow, U.K., Mar. 2024, pp. 1–5, doi: 10.23919/eucap60739.2024.10501149.

[25] T. Djerafi, N. J. G. Fonseca, and K. Wu, "Broadband substrate integrated waveguide 4 × 4 Nolen matrix based on coupler delay compensation," *IEEE Trans. Microw. Theory Techn.*, vol. 59, no. 7, pp. 1740–1745, Jul. 2011.

[26] F. E. Fakoukakis and G. A. Kyriacou, "Novel Nolen matrix based beamforming networks for series-fed low SLL multibeam antennas," *Prog. Electromagn. Res. B*, vol. 51, pp. 33–64, 2013, doi: 10.2528/pierb13011605.

[27] Q. Li, J. Hirokawa, T. Tomura, and N. J. G. Fonseca, "Two-dimensional one-body 3 × 3-way hollow-waveguide Nolen matrix using a two-plane unequal division coupler," *IEEE Trans. Microw. Theory Techn.*, vol. 72, no. 1, pp. 376–390, Jan. 2023, doi: 10.1109/TMTT.2023.3291759.

[28] Q. Li, J. Hirokawa, T. Tomura, Y. Takahashi, N. Kita, and N. J. G. Fonseca, "A two-dimensional 6 × 4-way hollow waveguide beam-switching matrix," *IEEE Access*, vol. 11, pp. 74239–74249, 2023, doi: 10.1109/access.2023.3296477.

[29] Y. J. Guo, M. Ansari, and N. J. G. Fonseca, "Circuit type multiple beamforming networks for antenna arrays in 5G and 6G terrestrial and non-terrestrial networks," *IEEE J. Microw.*, vol. 1, no. 3, pp. 704–722, Jul. 2021, doi: 10.1109/JMW.2021.3072873.

[30] Q.-L. Yang, Y.-L. Ban, J.-W. Lian, Z.-F. Yu, and B. Wu, "SIW Butler matrix with modified hybrid coupler for slot antenna array," *IEEE Access*, vol. 4, pp. 9561–9569, 2016, doi: 10.1109/ACCESS.2016.2645938.

[31] M. W. Almeshehe, N. A. Murad, M. K. A. Rahim, O. Ayop, F. Zubir, M. Z. A. A. Aziz, M. N. Osman, and H. A. Majid, "Low loss waveguide-based Butler matrix with iris coupling control method for millimeterwave applications," *Waves Random Complex Media*, vol. 33, no. 2, pp. 372–392, Feb. 2021.

HATEM ODAY HANOOSH was born in Samawah, Iraq, in 1991. He received the B.S. degree in computer techniques engineering from Islamic University College, Najaf, in 2014, the master's degree in electronic engineering (telecommunication system) from Universiti Teknikal Malaysia Melaka (UTeM), Malaysia, in 2018, and the Ph.D. degree in communications and waveguide Nolen matrix on millimeter-wave from Universiti Teknologi Malaysia (UTM), Johor Bahru, in 2023. His currently a Professor with the Engineering Electronics and Communication Department, Al-Muthanna University. His research interests include the design of antennas, dielectric resonator antennas, waveguide antennas, reflectarray antennas, Nolen matrix, and design for slot antennas.

MOHAMAD KAMAL A. RAHIM (Senior Member, IEEE) was born in Alor Setar, Kedah, Malaysia, in 1964. He received the B.Eng. degree in electrical and electronic engineering from the University of Strathclyde, U.K., in 1987, the master's degree in engineering from the University of New South Wales, Australia, in 1992, and the Ph.D. degree in wideband active antenna from the University of Birmingham, U.K., in 2003. From 1992 to 1999, he was a Lecturer with the Faculty of Electrical Engineering, Universiti Teknologi Malaysia, where he was a Senior Lecturer with the Department of Communication Engineering, from 2005 to 2007. He is currently a Professor with Universiti Teknologi Malaysia. His research interests include the design of active and passive antennas, dielectric resonator antennas, microstrip antennas, reflectarray antennas, electromagnetic bandgap, artificial magnetic conductors, left-handed metamaterials, and computer-aided design for antennas.

NOOR ASNIZA MURAD (Senior Member, IEEE) received the degree in electrical engineering majoring in telecommunication and the master's degree in engineering from the Universiti Teknologi Malaysia (UTM), in 2001 and 2003, respectively, and the Ph.D. degree, in 2011, for research on micromachined millimeter-wave circuits under supervision of Prof. Lancaster. She joined the Department of Radio Communication Engineering (RaCED), Faculty of Electrical Engineering (FKE), UTM, as a Tutor. She was appointed as a Lecturer, in April 2003. She joined the Emerging Device Technology Group, University of Birmingham, U.K. She was with HID GLOBAL Sdn Bhd for one year under Research and Development specifically working on RFID tag design, testing, and development. She is leading the Advance RF and Microwave Research Group, School of Electrical Engineering, UTM. Her research interests include antenna design for RF and microwave communication systems, millimeter-wave circuits design, RFID, and antenna beamforming. She is a member of the Antenna and Propagation (AP/MTT/EMC) Malaysia Chapter.

YAQDHAN MAHMOOD HUSSEIN was born in Samawah, Iraq, in 1991. He received the B.S. degree in computer techniques engineering from Islamic University College, Najaf, in 2015, and the M.S. degree in electronic engineering (telecommunication system) from Universiti Teknikal Malaysia Melaka (UTeM), Malaysia, in 2018. He is currently pursuing the Ph.D. degree in electronic engineering with Universiti Teknologi Malaysia (UTM), Johor Bahru. His current research interests include millimeter wave antennas, base station antennas, and SIW technology with butler matrix.